

LSTM-based Selective Dense Text Retrieval Guided by Sparse Lexical Retrieval

Yingrui Yang¹[0000-0001-6454-5796], Parker Carlson²[0000-0003-1856-5088],
Yifan Qiao³[0000-0001-5717-2637], Wentai Xie²[0009-0007-7870-3100],
Shanxiu He²[0009-0008-8581-6733], and Tao Yang²[0000-0003-1902-3387]

¹ Coursera Inc., USA, yingruiyang@ucsb.edu

² University of California at Santa Barbara, USA, {parker_carlson, wentaixie,
shanxiuhe, tyang}@ucsb.edu

³ Apple Inc., USA, yifan-qiao@apple.com

Abstract. This paper studies fast fusion of dense retrieval and sparse lexical retrieval, and proposes a cluster-based selective dense retrieval method called CluSD guided by sparse lexical retrieval. CluSD takes a lightweight cluster-based approach and exploits the overlap of sparse retrieval results and embedding clusters in a two-stage selection process with an LSTM model to quickly identify relevant clusters while incurring limited extra memory space overhead. CluSD triggers partial dense retrieval and performs cluster-based block disk I/O if needed. This paper evaluates CluSD and compares it with several baselines for searching in-memory and on-disk MS MARCO and BEIR datasets.

Keywords: Partial dense retrieval, selective fusion with sparse retrieval, efficient document search

1 Introduction and Related Work

Dense and sparse retrievers are two main categories of retrieval techniques for text document search. As shown in previous literature [21, 24, 25], combining sparse and dense retrieval scores with linear interpolation can boost search relevance. It is important to optimize for efficiency when combining the above two retrieval approaches on a low-cost CPU-only platform. This is desirable in a large-scale search system which employs a multi-stage search architecture, and runs partitioned first-stage retrieval in parallel on a massive number of inexpensive CPU-only machines. It is also critical for search on personal devices such as phones with limited computing/memory resources or battery use constraints.

Dense retrieval can be accelerated with approximate nearest neighbor (ANN) search using partial IVF cluster search [18, 23] or proximity-graph-based navigation (e.g. HNSW) [29]. However, there is a significant relevance tradeoff for a reduced search cost in these efforts. For example, RetroMAE [41], a state-of-the-art dense retriever, is slow on CPU without compression, the use of 5% IVF cluster search reduces CPU time substantially, but there is a 7.5% drop in MRR@10. The use of OPQ quantization [13], implemented in FAISS [18], further

reduces memory space to 1.2GB but causes an extra 4.6% MRR@10 drop. Notice that the idea of cluster-based retrieval was explored for traditional information retrieval and selective search [1, 4, 15].

LADR [20], as a follow-up study of GAR [28], has investigated partial dense retrieval by using the results of a sparse retriever as a seed to select embeddings based on a document-to-document proximity graph. This strategy follows the previous graph-based ANN approaches [29, 36]. Using sparse retrieval results as a seed allows quick narrowing of the search scope at a low CPU cost. While LADR and HNSW have demonstrated their high efficiency to search within a time budget, the use of a document-wise similarity graph adds a significant online space requirement on a low-cost computing platform. For example, the proximity graph can take an extra 4.3GB of memory space [20] for 8.8M MS MARCO passages.

Another limitation of LADR and HNSW is the assumption of in-memory access to proximity graphs and dense vectors. For large datasets or higher-dimension embedding vectors, some or all of the embeddings and proximity graphs will have to be stored on disk, especially when such applications desire uncompressed embeddings for better relevance. For example, the embedding dimension of the recent RepLLaMA dense retriever [27] is 4096, based on LLaMA-2 [38], which leads to 145GB storage space for MS MARCO passages. It is possible that more advanced dense models may be developed to take advantages of large language models in the future with a higher embedding dimensionality (e.g. up to 12,288 [2]) for better relevance. For large on-disk search, random access of dense embeddings and/or a document-level proximity graph can incur substantial fine-grained I/O overhead. DiskANN [17] and SPANN [5] are two on-disk ANN search algorithms for general data applications which do not leverage sparse retrieval. They have not been studied in the context of text document retrieval where the importance of semantic text matching presents a unique challenge and requires new design considerations.

One recently published contemporary work, CDFS [42], addresses the above problem. One weakness of CDFS is that it uses probabilistic thresholding to select dense clusters based on a strong assumption that the order statistics of query document ranking is independently and identically distributed. This assumption is only true when the query document similarity scores for relevant and irrelevant documents follow the same distribution, which is rare because they are usually distributed differently.

This paper proposes a lightweight approach called CluSD (Cluster-based Selective Dense retrieval) guided by sparse retrieval results. Unlike CDFS, CluSD does not follow any statistical distribution assumption. CluSD limits query-document similarity computations through a two-stage cluster selection algorithm via an LSTM model, which exploits inter-cluster distances and the overlapping degree between top sparse retrieval results and dense clusters. When dense clusters are not available in memory, CluSD selects and loads a limited number of clusters with efficient disk block I/O. Thus, it can handle a large dataset with high-dimension embeddings that cannot fit in memory, with less I/O overhead compared to a graph-based ANN approach.

2 Selective Dense Cluster Retrieval

Problem definition. Given query q for searching a collection of D text documents: $\{d_i\}_{i=1}^D$, retrieval obtains the top k relevant documents from this collection based on the similarity between query q and document d_i using their representation vectors. With a lexical representation, each representation vector of a document or a query is sparse. Sparse retrieval uses the dot product of their lexical representation vectors as the similarity function and implements its search efficiently using an inverted index: $L(q) \cdot L(d_i)$ where $L(\cdot)$ is a lexical representation which is a vector of weighted term tokens for a document or a query. For BM25-based lexical representation [34], $L(\cdot)$ treats each document or a query as a bag of terms. Term weights are scaled based on the frequency of terms within a document and across all documents in the collection. For a learned sparse representation [8, 11, 25, 30], a document or a query is encoded using a trained neural ranking model, which produces modified representations of document or query containing both original and expanded terms. The encoding functions for a query and document can be different. Without the loss of generality, we assume they are the same in this paper. With a single-vector dense representation, each representation vector of a document or a query is a dense vector. Dense retrieval computes the following rank score: $R(q) \cdot R(d_i)$ where $R(\cdot)$ is a dense representation vector of a fixed size [19].

Following the work of [12, 21, 24], linear interpolation is used to ensemble dense and sparse retrieval scores. The fused rank score for document d_i in responding query q is: $\alpha L(q) \cdot L(d_i) + (1 - \alpha) R(q) \cdot R(d_i)$ where α is a coefficient in a range between 0 and 1. Our goal is to maintain a relevance competitive to full dense retrieval, while minimizing the time and memory overhead of cluster-based dense retrieval, guided by sparse retrieval results.

Design considerations. We aim to identify the opportunity to skip a substantial portion of dense retrieval by taking the IVF clustering approach [18] that groups similar documents. This helps CluSD to recognize similar relevant documents during inference while avoiding the need of a document-level proximity graph. The number of clusters needs to be as large as possible (meaning a small size per cluster) to avoid unnecessary I/O and computing cost. That imposes a significant challenge for accurate and fast selection of dense clusters. To address this our work proposes a two-stage LSTM-based selection algorithm that exploits the overlap of sparse retrieval results with the potential dense clusters.

2.1 Steps of online inference in CluSD

Online inference of CluSD has the following steps: **Step 1:** Conduct sparse retrieval to obtain top- k results. **Step 2:** Conduct a two-stage selection process. Stage I selects the top- n clusters from the given N dense embedding clusters, discussed in detail in Section 2.2. Stage II applies an LSTM model to the n top clusters to choose a limited number of dense clusters to evaluate, discussed in Section 2.3. **Step 3:** Expand the top- k sparse retrieval results to include the

documents vectors of these dense clusters and fuse their sparse and dense scores with linear interpolation.

Time and space cost for CluSD. The embedding space is $O(D)$ for a corpus with D vectors. For MS MARCO, this cost is around 27GB without compression. Quantization can reduce the total size to about 0.5GB to 1GB, depending on codebook parameters. Then this cost becomes a fraction of sparse retrieval index cost. Excluding embeddings, the extra space overhead for CluSD is to maintain the similarity among centroids of N clusters. We only maintain the top m cluster neighbors for each cluster in terms of their centroid similarity. For our evaluation, $m = 128$ and this reduces the extra space overhead as $O(N)$, which is negligible compared to the embedding space with $N \ll D$. For example, with $N = 8192$, the inter-cluster graph for MS MARCO passages takes about 5MB with quantization. Excluding sparse retrieval cost, the time cost of CluSD is dominated by the cost of cluster selection and dense similarity computation of selected dense clusters. The former is about $O(n)$ while the latter is proportional to the number of clusters selected, which is capped by $O(\frac{D}{N}n)$. In our evaluation of MS MARCO and BEIR, n is chosen to be 32, and the actual number of clusters selected and visited is about 22.3. Thus, the overall latency time overhead introduced by CluSD is fairly small.

2.2 Stage I of Step 2: Selection of top n candidate clusters

Given N clusters grouped using dense document embeddings, we devise a strategy to conduct a preliminary selection that prunes low-scoring clusters that contain only less relevant documents. A two-stage approach is motivated by the fact that it is too time consuming for an LSTM model, used in the second stage, to examine all clusters. Thus, we choose the top- n candidate clusters first.

To prioritize clusters, one idea is to adopt their query-centroid distance used in IVF cluster selection. We find this does not work well for CluSD. For example, if we rank clusters based on the query-centroid distance for MS MARCO passages, around 10% of top-10 dense results reside in clusters ranked beyond the 175th cluster, which means we would have to select 175 clusters in order to recover 90% of top-10 documents. Visiting all of these clusters is still too slow and CluSD only visits about 22.3 clusters on average for MS MARCO Dev set.

Our method for the preliminary selection at this stage is to rely on the degree of overlap between dense clusters and the top sparse retrieval results. Specifically, we divide k top sparse retrieval results into v top sparse result bins denoted B_1, \dots, B_v . We assign each embedding cluster C_i with a priority vector $(P(C_i, B_1), \dots, P(C_i, B_v))$ where $P(C_i, B_j) = |C_i \cap B_j|$, which is the number of documents in top sparse bin B_j included in cluster C_i . A larger $P(C_i, B_j)$ value indicates a higher priority for C_i with respect to sparse result position bin B_j . In our evaluation with retrieval depth $k = 1000$ for the MS MARCO and BEIR datasets, we use $v = 6$ result bins, divided into the top-10 results, top 11-25, top 26-50, top 51-100, top 101-200, top 201-500, and top 501 to k documents. The main reason to divide sparse results into bins is to reduce the time complexity of LSTM for cluster selection with a shorter sequence. The

reason to have a non-uniform bin size is that the importance of rank positions derived by sparse retrieval is nonlinear. For example, the top 1 to 50 results are much more important than the results ranked from 50 to 1,000, requiring finer grained partitioning. Then, we perform multikey sorting based on cluster priority vectors $(P(C_i, B_1), \dots, P(C_i, B_v))$. The clusters are sorted first based on $(P(C_i, B_1))$, then $(P(C_i, B_2))$ if there's a tie. If there is a tie between two clusters, then we rank them by their centroid distance to the query. The top- n ranked candidate clusters will be the input for the LSTM model described below.

2.3 Stage II of Step 2: Selection with LSTM

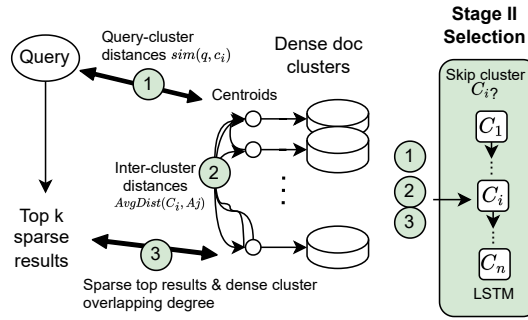


Fig. 1. Illustration of CluSD and its features.

To select which dense clusters we visit, we adopt a simple LSTM model [16] which takes a sequence of clusters as input along with their features. We choose an LSTM because it can capture cluster selection order as a sequence. Selected clusters can influence what will be selected next based on their semantic distance and other features. This allows CluSD to select clusters accurately to minimize I/O and computing cost. The time complexity of the LSTM model is limited by $O(n)$, where the n top clusters are given from Stage I.

The LSTM sequentially visits each cluster, denoted C_1 to C_n . For each cluster C_i , the LSTM predicts a score $f(C_i)$ such that $0 \leq f(C_i) \leq 1$. If $f(C_i) \geq \theta$, where θ is a set prediction threshold, then cluster C_i should be visited. θ controls the tradeoff between efficiency and relevance; in practice, θ can be tuned based on the overall latency requirement. In our experiments, the default setting of CluSD is to use a threshold of 0.02, yielding 22.3 clusters selected on average. Due to the page limit, we have omitted a study of the impact of varying this threshold on the number of clusters selected.

As depicted in Figure 1, the feature input vector for the current cluster C_i for the above LSTM computation to produce $f(C_i)$ is composed of the following three groups of features:

- **Query-cluster similarity:** $sim(q, c_i)$. The similarity distance of this query q with the centroid c_i of cluster C_i .
- **Inter-cluster similarity:** $AvgDist(C_i, A_j)$ for $1 \leq j \leq u$. Given the n sorted clusters derived from Stage I, we uniformly partition these n consecutive clus-

ters into u consecutive cluster bins: $\{A_1, A_2, \dots, A_u\}$. Then we define

$$AvgDist(C_i, A_j) = \frac{1}{|A_j|} \sum_{c_l \in A_j} sim(c_i, c_l)$$

where c_l is the centroid representing cluster C_l in bin A_j . The above formula computes the mean distance between centroid c_i and the centroid of each cluster within Bin A_j .

The purpose of this feature group is to capture the distances of a cluster to previously examined clusters and unexamined clusters following the LSTM flow. When the mean distance between cluster c_i and clusters in a previously-examined bin is close, if many clusters in that bin have been selected, cluster c_i may have a good chance to be selected. In our evaluation with MS MARCO and BEIR datasets, we found that $u = 6$ is appropriate. As discussed earlier in Section 2.1, to reduce the extra space cost, we only maintain top- m cluster neighbors of each cluster where m is not large (128 in our evaluation).

- **Cluster overlap:** $P(C_i, B_j)$ and $Q(C_i, B_j)$ for $1 \leq j \leq v$.

This group of features captures the position-weighted and score-weighted overlap degree of this embedding cluster C_i with the top sparse results. Stage I in Section 2.2 divided the top- k sparse retrieval results into v position bins B_1, \dots, B_v and defined $P(C_i, B_j)$ as the count-based overlap measure. Now, we define a score-weighted overlap degree $Q(C_i, B_j)$ as the average sparse rank score of documents that are in both C_i and sparse position bin B_j . Namely,

$$Q(C_i, B_j) = \frac{\sum_{d \in C_i \cap B_j} SparseRankScore(d)}{|C_i \cap B_j|}.$$

Clusters with high Q scores for the top bins contain many top sparse results and may be selected.

Training of LSTM. We assume that the training data contains a set of queries and relevance-labeled documents, that allows the computation of a ranking metric such as MRR or NDCG. For example, from MS MARCO training set we randomly sample 5000 training instances, where each training instance contains a query and one or more relevant documents. To train the LSTM for cluster selection, for each training instance, we mark the positive and negative examples for top cluster selection. If a cluster contains one of top-10 dense retrieval results, we mark this cluster as positive otherwise negative. This approximately indicates that such an embedding cluster should be visited for a fusion.

3 Evaluations

Datasets and measures. Our evaluation uses the MS MARCO dataset with 8.8 million passages [3, 7] for training and in-domain search, and the 13 publicly available BEIR datasets [37] for zero-shot retrieval. The size of BEIR data sets ranges from 3,633 to 5.4M documents. To report the mean latency and 99 percentile latency, we test queries multiple times using a single thread on a 2.25GHz AMD EPYC 7742 CPU server with PCIe SSD.

Models and parameters. For sparse retrieval, we use SPLADE [9, 10, 22] with hybrid thresholding [32] and BM25-guided traversal [31, 33]: 1) SPLADE-HT1 with index space 3.9GB and 31.2 ms retrieval latency. We also test on three other sparse models: 2) uniCOIL [11, 25] with 1.2GB index and 35.5ms latency; 3) LexMAE [35] with 3.7GB index and 180ms latency; 4) BM25-T5 that applies BM25 with DocT5Query document expansion [6]. BM25-T5 has a 1.2GB index and 9.2ms latency. For dense retrieval, we adopt the recent dense models SimLM [39], RetroMAE [41], and RepLLaMA [27]. We use K-means in the FAISS library [18] to derive dense embedding clusters. RetroMAE-2 [26] is not used because its checkpoint is not released.

Our evaluation implementation uses C++ and Python. To train the CluSD model, we sample 5000 queries from the MS MARCO training set and the hidden dimension for LSTM is 32. The models are trained for 150 epochs. For sparse and dense model interpolation, we use min-max normalization to rescale the top results per query. For BM25-T5, the interpolation weights are 0.05 and 0.95 for sparse and dense scores, respectively. For other sparse retrieval models, they are 0.5 and 0.5. The results are marked with tag \dagger when statistically significant drop is observed compared to the baseline marked with \blacktriangle at 95% confidence level.

Time budget. We mainly use a time budget of about 50ms including the sparse retrieval time for the average latency, and the use of this budget allows us to choose the algorithm parameters accordingly. We choose this budget because in a search system running as an interactive web service, a query with multi-stage processing needs to be completed within a few hundred milliseconds. A first-stage retriever operation for a data partition needs to be completed within several tens of milliseconds without query caching.

Table 1. Cluster-based in-memory search with and without space constraints

	% D	MSMARCO Dev		DL19	DL20	BEIR	Latency ms
		MRR@10	R@1K	NDCG@10	NDCG@10	NDCG@10	
Uncompressed flat setting. Embedding space 27.2GB							
D=RetroMAE	100	0.416 \dagger	0.988	0.720	0.703	0.482	1674.1
\blacktriangle S + D	100	0.425	0.988	0.740	0.731	0.520	1705.3
S + CDFS	0.45	0.424	0.987	-	-	0.517	46.0
S + CluSD	0.3	0.426	0.987	0.744	0.734	0.518	44.4
OPQ $m = 128$. Embedding space 1.1GB							
\blacktriangle S + D-OPQ	100	0.416	0.988	0.737	0.732	0.515	600.1
S+D-IVF	10	0.404 \dagger	0.987	0.713	0.722	0.513	126.4
S+D-IVF	5	0.394 \dagger	0.987	0.687	0.706	0.507	80.0
S+D-IVF	2	0.374 \dagger	0.986	0.656	0.700	0.499	52.5
S+CDFS	0.45	0.415	0.986	0.740	0.730	-	43.3
S + CluSD	0.3	0.417	0.986	0.742	0.735	0.514	42.6

Cluster-based retrieval with in-memory data. Table 1 compares CluSD with a few baselines for cluster-based selective retrieval in searching MS MARCO and BEIR datasets with and without compression. The dense model is RetroMAE and sparse model is SPLADE-HT1. IVFOPQ uses a proportion of top dense clusters sorted by the query-centroid distance. OPQ quantization from FAISS is configured with the number of codebooks as $m = 128$ or 64. We report performance of IVF clustering using the top 10%, 5%, or 2% clusters respec-

tively. The notation “S+D” in Table 1 (and later in other tables) reports the fused performance of a sparse model with linear interpolation. Marker “%D” means the approximate percentage of document embeddings evaluated based on the number of clusters selected. The last column marked with “Latency” is the mean single-query time for MS MARCO Dev set. CluSD uses setting $N = 8192$ and $n = 32$, which results in selection of 22.3 clusters on average per query and allows CluSD to meet the latency requirement. The results in Table 1 shows that under the same time budget, CluSD outperforms partial dense retrieval with IVF search in relevance. Additionally, CluSD performs slightly better than CDFS in terms of both relevance and latency because CluSD’s LSTM effectively selects less clusters to search than CDFS.

CluSD vs. graph navigation. Table 2 compares CluSD with selective dense retrieval based on proximity graph navigation including HNSW and LADR under time budget around 50ms. HNSW’s expansion factor parameter (ef) is set as 1024. For LADR, we use its default setting with seed = 200, number of neighbors = 128 and use an exploration depth of 50 to meet the latency budget. The takeaway from this table is that relevance of CluSD is better than HNSW while CluSD has similar or slightly better relevance without incurring significant extra space cost, compared to LADR. When the time budget is around 25ms, the takeaway is similar.

Table 2. CluSD vs. graph navigation methods

	MSMARCO Dev		DL19	DL20	Latency Space	
	MRR@10	R@1K	NDCG	NDCG	Total(ms)	GB
Time Budget = 50 ms, S=SPLADE-HT1						
D=SimLM	0.411 [†]	0.985 [†]	0.714	0.697	1674.1	27.2
S	0.396 [†]	0.980 [†]	0.732	0.721	31.2	3.9
▲ S + D	0.424	0.989	0.740	0.726	1705.0	31.1
HNSW	0.409 [†]	0.978 [†]	0.669	0.695	54.4	40.3
S + HNSW	0.420	0.987	0.718	0.723	59.6	40.3
S + LADR	0.422	0.984 [†]	0.743	0.728	43.6	35.4
S + CluSD	0.426	0.987	0.744	0.724	46.3	31.1

Table 3. Zero-shot performance in average NDCG@10 on BEIR datasets.

	SPLADE			SPLADE-HT1+SimLM				SPLADE-HT1+RetroMAE							
	BM25	SimLM	RetroMAE	-HT1	▲ flat	rrk	flat	m=128	m=64	▲ flat	rrk	flat	flat	m=128	m=64
Avg.	0.440	0.429	0.482	0.500	0.518	0.496	0.516	0.514	0.511	0.520	0.483	0.517	0.518	0.514	0.506

Detailed zero-shot performance with BEIR. Table 3 lists the performance of CluSD with SimLM and RetroMAE after SPLADE-HT1 retrieval in searching each of 13 BEIR datasets. The LSTM model of CluSD is trained with the MS MARCO training set, and it is directly applied to each BEIR dataset to select clusters without further tuning. As a baseline, column “▲ flat” is to fuse the uncompressed full dense retrieval with SPLADE-HT1 sparse retrieval. Column marked “rrk” is to rerank top 1,000 sparse retrieval results interpolated with

their dense scores. Columns with “CluSD-flat”, “CluSD-m=128” and “CluSD-m=64” are CluSD results using uncompressed or compressed embeddings with m=128 or m=64. This table also includes a column marked with “CDFS-flat” which is the selective fusion outcome with CDFS using uncompressed RetroMAE embeddings.

Table 3 shows that the relevance of CluSD with selective fusion of sparse and dense results is higher than each individual retriever, and CluSD with limited dense retrieval performs closely to oracle “▲ flat”, and delivers good NDCG@10 under two compression settings. CluSD is competitive to CDFS for the fusion of SPLADE and RetroMAE.

CluSD vs. baselines with in-memory or on-disk data. Table 4 examines the performance of CluSD fused with SPLADE when MS MARCO passage embeddings cannot fit in memory and are stored on an SSD disk. We use $N = 65,000$ for CluSD, and the extra space for quantized inter-cluster distances takes about 40MB. This setting here is larger than the $N = 8192$ setting in Table 1 and we choose that because a smaller cluster size gives a flexibility in reducing the disk I/O size when the total number of clusters selected by CluSD is controlled. We also compare other selective dense retrieval baselines using reranking or proximity graph navigation. The mean response time (MRT) and 99th percentile (P99) include the total sparse and dense retrieval time for methods noted “S+*”, otherwise only the dense retrieval time. The MRT cost breakdown for I/O and CPU time is also listed. Times reported are in milliseconds. “%D” is the approximate percentage of document embeddings evaluated based on the number of clusters fetched from the disk.

Reranking simply fetches top- k embeddings from the disk for fusion. LADR is designed for in-memory search [20] and we run it by assuming memory can sufficiently host the proximity graph while letting LADR access embeddings from the disk. Excluding the I/O cost portion of LADR in this table, the in-memory search cost of LADR is marked in the “CPU” column. We test two configurations of LADR, its default with 128 neighbors, 200 seed documents, and a search depth of 50, as well as a faster configuration, selected such that its CPU time is similar to CluSD. LADR_{fast} uses 128 neighbors, 50 seed documents, and a depth of 50. DiskANN [17] assumes the graph and original embeddings are on disk while the memory hosts compressed embeddings for quick guidance. SPANN [5] searches disk data in a cluster-based manner based on query-centroid distances. Both DiskANN and SPANN are designed for on-disk search from scratch without fusing with others, and thus we simply fuse their outcome with SPLADE results. HNSW [29] is not included because its in-memory relevance is similar as DiskANN while it is not designed to be on disk.

CluSD significantly outperforms all other methods by leveraging block I/O. CluSD is 2.2x faster than the next fastest system (SPANN), while having a noticeably higher relevance. DiskANN performs similarly to SPANN in terms of relevance, but is 4.97x slower than CluSD. Reranking has a lower MRR@10 and recall@1k while being 2.85x slower. Both variants of LADR have a lower MRR@10 than CluSD, but are 6.2x and 12.1x slower on average for LADR_{fast}

Table 4. Search when uncompressed embeddings are on disk for SPLADE + SimLM

S=SPLADE-HT1	%D	Relevance		Latency (ms)		Breakdown	
		MRR@10	R@1K	MRT	P99	I/O	CPU
S+Rerank	0.01	0.421	0.980 [†]	158.7	217.3	125.2	33.5
S+LADR _{fast}	0.03	0.419	0.980 [†]	346.1	1013	1003	41.5
S+LADR _{default}	0.10	0.422	0.984	674.9	2849	2788	61.3
DiskANN	–	0.398 [†]	0.970 [†]	276.5	321	272	5.2
S+ DiskANN	–	0.417 [†]	0.984	307.7	352.2	272	36.4
SPANN	–	0.396 [†]	0.965 [†]	123.6	159.6	–	–
S+SPANN	–	0.420	0.989	154.8	190.8	–	–
▲ S+CluSD	0.05	0.425	0.986	55.6	94.4	17.5	38.1

and LADR_{default} respectively. We find that each I/O operation has about a 0.15ms queuing and other software overhead on our tested PCIe SSD. Thus, more fine-grained operations in reranking yields more overhead. Proximity graph methods such as LADR rely on large amounts of fine-grained I/O operations and suffer significantly in terms of latency when embeddings are stored on disk. In comparison, CluSD takes advantage of block I/O operations because it fetches documents by clusters and thus CluSD issues fewer I/O requests to search more documents in less time.

CluSD with LLaMA-2 based dense retrieval. Table 5 demonstrates that CluSD effectively supports selective RepLLaMA dense retrieval [27] to take advantage of LLMs on CPUs. The “Latency” column includes sparse retrieval CPU time when “S+” is marked in the method name. S=SPLADE-HT1. RepLLaMA uses 145GB embedding space with 4K dimensionality. All rows except the last row conduct in-memory search assuming data fits into memory. Row 1 shows it takes 7.9 second CPU time to conduct in-memory full RepLLaMA retrieval. Row 2 shows performance of RepLLaMA using OPQ quantization but without IVF selective search. Row 3 shows performance of RepLLaMA using OPQ and IVF selective search. Use of these optimization techniques leads to a significant relevance degradation. As a reference, Row 4 lists the fusion of SPLADE and full dense retrieval. CluSD visits a small number of clusters from the 60,000 dense RepLLaMA clusters. CluSD with SPLADE-HT1 takes about 39ms for in-memory search shown in Row 6, and 60ms with on-disk search shown in Row 8. RepLLaMA inference requires five Nvidia 32GB V100 GPUs to host data and take 37ms GPU time. Thus, CluSD can deliver 1 to 2 orders of magnitude of improvement in either total latency or infrastructure cost. Rows 5 and 7 show the performance of CDFS, which is similar to CluSD for in-memory search, but 23.3% slower than CluSD for on-disk search while achieving a similar relevance.

For the BEIR datasets, RepLLaMA achieves an average NDCG of 0.561. While significantly faster than RepLLaMA, CluSD achieves an average NDCG of 0.541 while CDFS reaches 0.554. However, CluSD’s LSTM model for RepLLaMA was used in a zero-shot manner after being trained using SimLM on MS MARCO passage. In the future we expect that further improvement in CluSD is possible if its LSTM is trained using RepLLaMA.

Table 5. Selective fusion with dense RepLLaMA and sparse SPLADE

	Method	MRR@10	R@1K	Latency	Space
1.	RepLLaMA	0.412 [†]	0.990	7.9 s	145 GB
2.	RepLLaMA-OPQ	0.384 [†]	0.990	666 ms	2.4 GB
3.	RepLLaMA-IVFOPQ	0.365 [†]	0.915 [†]	97 ms	6.1 GB
4.	S + RepLLaMA	0.426	0.994	7.9 s	149 GB
5.	S+CDFS	0.425	0.987	41 ms	149 GB
6.	S+CluSD	0.424	0.986	39 ms	149 GB
7.	S+CDFS (on-disk)	0.425	0.987	74 ms	149 GB
8.	▲ S+CluSD (on-disk)	0.424	0.986	60 ms	149 GB

CluSD with other sparse models and quantization methods. Table 6 examines CluSD’s fusion of SimLM with other three sparse models. Last column lists in-memory dense retrieval portion of latency. For each sparse model, CluSD boosts overall relevance. As CluSD’s cluster selection relies on the overlap feature of top sparse results with dense clusters, the guidance from the fastest BM25 results is less accurate than other sparse models. On the other hand, with a guidance from the slowest but stronger LexMAE retrieval, CluSD yields the highest MRR@10, comparable to full search.

Table 6. CluSD with LexMAE, uniCOIL & BM25 sparse models

Sparse model	LexMAE		uniCOIL		BM25T5		Dense
	MRR	R@1K	MRR	R@1K	MRR	R@1K	latency
Uncompressed SimLM embeddings with 27.2 GB space							
S	0.425	0.988	0.347 [†]	0.957 [†]	0.259 [†]	0.935 [†]	-
▲ S + D	0.430	0.990	0.413	0.985	0.415	0.985	1674ms
S + Rerank	0.432	0.988	0.415	0.957 [†]	0.409	0.935 [†]	21.9ms
S + CluSD	0.431	0.989	0.414	0.980	0.410	0.980	12.1ms
OPQ m=128. SimLM embedding space 1.1 GB							
S + D-IVFOPQ	0.383 [†]	0.988	0.354 [†]	0.961 [†]	0.369 [†]	0.975 [†]	21.9ms
S + CluSD	0.429	0.989	0.404	0.980	0.402 [†]	0.975 [†]	9.8ms

CluSD with advanced quantization models. Table 7 shows the use of two other recent quantization methods DistillVQ [40] and JPQ [43] with in-memory CluSD for MS MARCO Passage Dev set. For JPQ, we use its released model and compression checkpoints and follow its default setting with $m = 96$. For DistillVQ, we use its released code to train compression on the RetroMAE model using its default value $m = 128$. While switching to a different quantization affects compression and relevance, this result shows that CluSD is still effective and outperforms other baselines.

Table 7. Use of CluSD with DistillVQ and JPQ quantization

Quantization	DistillVQ			JPQ		
S=SPLADE-HT1	MRR@10	R@1K	Latency	MRR@10	R@1K	Latency
IVF (2%)	0.365 [†]	0.899 [†]	20.8 ms	0.326 [†]	0.917 [†]	21.3 ms
S+ IVF (2%)	0.392 [†]	0.987	52.0 ms	0.379 [†]	0.985	52.5 ms
▲ S+CluSD	0.417	0.987	40.9 ms	0.392	0.985	42.4 ms

Design options for CluSD. Table 8 investigates the impact of the following design options for cluster selection in CluSD with the MS MARCO Dev set. For Stage I selection, we explore two options: 1) SortByDist: Choose top clusters sorted by the distance of their centroids to the query embedding. 2) SortByOverlap: Choose top clusters sorted by $P(C_i, B_j)$ features discussed in Section 2. Namely, use the overlap degree of clusters with top result bins of sparse retrieval. For Stage II selection, we explore three options: 1) XGBoost: Use the boosting tree XGBoost model to detect if a cluster should be visited. The features used are the same ones discussed in Section 2. This is a pointwise approach, as we view query-cluster pairs as independent samples, and the decision on one cluster does not affect other clusters for the same query. 2) RNN: Use a vanilla RNN model. The feature and sequence setup is the same as our LSTM model. 3) LSTM: the model we used in CluSD. We also assess the impact of removing a feature group used in CluSD: 1) w/o inter-cluster dist: removing the inter-cluster distance feature group; 2) w/o S-C overlap: removing the overlap-degree feature of top sparse results with each cluster.

Table 8. Design options for CluSD. \blacktriangle is the default choice.

Avg #clusters targeted	3		5		Time ms
	MRR@10	R@1K	MRR@10	R@1K	
<i>Stage II is removed. Stage I options only</i>					
SortByDist	0.297	0.655	0.331	0.740	0
\blacktriangle SortByOverlap	0.384	0.867	0.401	0.917	0.2
<i>Stage I=SortByDist; Stage II model options</i>					
XGBoost	0.398	0.888	0.404	0.929	192
RNN	0.404	0.908	0.406	0.938	2.8
LSTM	0.406	0.923	0.406	0.943	2.8
<i>Stage II=SortByOverlap; Stage II LSTM feature group options</i>					
w/o inter-cluster dist	0.402	0.915	0.406	0.941	–
w/o S-C overlap	0.289	0.638	0.325	0.730	–
\blacktriangle Default	0.408	0.943	0.410	0.953	2.8

The last row marked “Default” is the final version used by CluSD with SortByOverlap and LSTM. To have a fair comparison, this table assumes on average either 3 or 5 clusters are targeted by CluSD. For XGBoost, RNN or LSTM, we set their prediction threshold so that the average number of clusters is close to the targeted number. The last column of this table is the time spent to select clusters. Table 8 shows that the RNN or LSTM based prediction achieves higher MRR@10 and recall compared to XGBoost. Feature exploration indicates that the overlap degree is important for cluster selection while the inter-cluster distance feature group is also useful.

Impact of cluster partitioning size. CluSD pre-partitions the embeddings into N clusters. Figure 2 shows the impact when N is 4096 and 8192 for MS MARCO Dev. Stage I of CluSD uses $n = 128$ in this figure. A solid line refers to the use of uncompressed dense embeddings while a dash-dot line refers to OPQ quantization with $m=128$, and a dotted line refers to OPQ quantization with

$m=64$. The x-axis is the average number of clusters selected by CluSD. We vary the selection threshold parameter Θ in CluSD to achieve the different average number of clusters selected. With both N values, MRR@10 exceeds 0.420 when more than 10 clusters are selected. As more clusters are selected, the recall ratio increases. Different N values impact latency. For example, when 10 clusters are selected on average, CluSD scans through 0.1% and 0.2% of embeddings, corresponding to $N=4096$ and 8192, respectively. When $N = 8192$, its latency is reduced because CluSD time complexity is proportional to the size per cluster and the number of clusters selected.

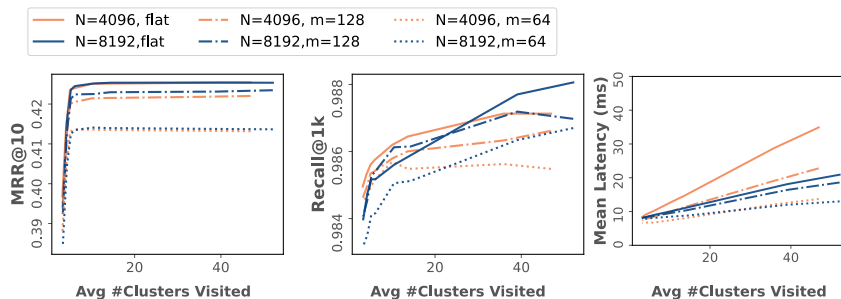


Fig. 2. CluSD relevance and latency vs. the average number of clusters selected

4 Concluding Remarks

CluSD is a lightweight cluster-based partial dense retrieval with fast CPU response time and competitive relevance. Compared to CDFS [42], CluSD does not make any strong statistical assumptions about the sparse ranking result distribution. The evaluation results show that CluSD can effectively select top dense clusters with a performance reasonably competitive to CDFS in relevance and latency even CluSD incurs small LSTM computing overhead. More studies and tuning could be conducted in the future in evaluating CluSD and CDFS.

The evaluation shows CluSD significantly outperforms cluster-based partial dense retrieval with IVF in relevance. Under the same time budget, CluSD with negligible extra space overhead delivers better or similar relevance than HNSW and LADR that rely upon a document-level proximity graph. Further, CluSD is up-to 12.1x faster than them when embeddings do not fit in memory. When compared to on-disk ANN methods DiskANN and SPANN [14, 17], CluSD is 2.2x and 4.97x faster respectively, while achieving better relevance by leveraging sparse retrieval. Compared to graph navigation approaches, CluSD does not need a document-level proximity graph, and it conducts faster block I/O when fetching clustered document embeddings from disk.

Acknowledgments. We thank anonymous referees for their valuable comments. This work is supported in part by U.S. NSF IIS-2225942 and has used the computing resource of the ACCESS program supported by NSF. Any opinions, findings, conclusions or recommendations expressed in this material are those of the authors and do not necessarily reflect the views of the U.S. NSF.

References

1. Altingovde, I.S., Demir, E., Can, F., Ulusoy, O.: Incremental cluster-based retrieval using compressed cluster-skipping inverted files. *ACM Trans. Inf. Syst.* **26**(3) (Jun 2008). <https://doi.org/10.1145/1361684.1361688>, <https://doi.org/10.1145/1361684.1361688>
2. Brown, T., Mann, B., Ryder, N., Subbiah, M., Kaplan, J.D., Dhariwal, P., Neelakantan, A., Shyam, P., Sastry, G., Askell, A., Agarwal, S., Herbert-Voss, A., Krueger, G., Henighan, T., Child, R., Ramesh, A., Ziegler, D., Wu, J., Winter, C., Hesse, C., Chen, M., Sigler, E., Litwin, M., Gray, S., Chess, B., Clark, J., Berner, C., McCandlish, S., Radford, A., Sutskever, I., Amodei, D.: Language models are few-shot learners. In: Larochelle, H., Ranzato, M., Hadsell, R., Balcan, M., Lin, H. (eds.) *Advances in Neural Information Processing Systems*. vol. 33, pp. 1877–1901. Curran Associates, Inc. (2020), https://proceedings.neurips.cc/paper_files/paper/2020/file/1457c0d6bfc4967418bfb8ac142f64a-Paper.pdf
3. Campos, D.F., Nguyen, T., Rosenberg, M., Song, X., Gao, J., Tiwary, S., Majumder, R., Deng, L., Mitra, B.: MS MARCO: A human generated machine reading comprehension dataset. *NIPS* (2016)
4. Can, F., Altingövde, I.S., Demir, E.: Efficiency and effectiveness of query processing in cluster-based retrieval. *Inf. Syst.* **29**, 697–717 (2004)
5. Chen, Q., Zhao, B., Wang, H., Li, M., Liu, C., Li, Z., Yang, M., Wang, J.: SPANN: Highly-efficient billion-scale approximate nearest neighborhood search. In: Beygelzimer, A., Dauphin, Y., Liang, P., Vaughan, J.W. (eds.) *Advances in Neural Information Processing Systems* (2021), <https://openreview.net/forum?id=-1rrzmJCp4>
6. Cheriton, D.R.: From doc2query to docttttquery (2019), <https://api.semanticscholar.org/CorpusID:208612557>
7. Craswell, N., Mitra, B., Yilmaz, E., Campos, D.F., Voorhees, E.M.: Overview of the trec 2020 deep learning track. *ArXiv abs/2102.07662* (2020)
8. Dai, Z., Callan, J.: Context-aware term weighting for first stage passage retrieval. *SIGIR* (2020)
9. Formal, T., Lassance, C., Piwowarski, B., Clinchant, S.: From distillation to hard negative sampling: Making sparse neural ir models more effective. *Proceedings of the 45th International ACM SIGIR Conference on Research and Development in Information Retrieval* (2022)
10. Formal, T., Piwowarski, B., Clinchant, S.: SPLADE: Sparse lexical and expansion model for first stage ranking. *SIGIR* (2021)
11. Gao, L., Dai, Z., Callan, J.: COIL: revisit exact lexical match in information retrieval with contextualized inverted list. *NAACL* (2021)
12. Gao, L., Dai, Z., Fan, Z., Callan, J.: Complementing lexical retrieval with semantic residual embedding. *ECIR abs/2004.13969* (2021)
13. Ge, T., He, K., Ke, Q., Sun, J.: Optimized product quantization for approximate nearest neighbor search. In: *Proceedings of the IEEE Conference on Computer Vision and Pattern Recognition (CVPR)* (June 2013)
14. Gollapudi, S., Karia, N., Sivashankar, V., Krishnaswamy, R., Begwani, N., Raz, S., Lin, Y., Zhang, Y., Mahapatro, N., Srinivasan, P., Singh, A., Simhadri, H.V.: Filtered-diskann: Graph algorithms for approximate nearest neighbor search with filters. In: *Proceedings of the ACM Web Conference 2023*. p. 3406–3416. WWW '23, ACM, New York, NY, USA (2023)

15. Hafizoglu, F., Kucukoglu, E., Altingövde, I.: On the efficiency of selective search. In: Proc. of ECIR 2017. pp. 705–712 (04 2017). https://doi.org/10.1007/978-3-319-56608-5_69
16. Hochreiter, S., Schmidhuber, J.: Long short-term memory. *Neural computation* **9**(8), 1735–1780 (1997)
17. Jayaram Subramanya, S., Devvrit, F., Simhadri, H.V., Krishnawamy, R., Kadekodi, R.: Diskann: Fast accurate billion-point nearest neighbor search on a single node. In: Wallach, H., Larochelle, H., Beygelzimer, A., d'Alché-Buc, F., Fox, E., Garnett, R. (eds.) *Advances in Neural Information Processing Systems*. vol. 32. Curran Associates, Inc. (2019), https://proceedings.neurips.cc/paper_files/paper/2019/file/09853c7fb1d3f8ee67a61b6bf4a7f8e6-Paper.pdf
18. Johnson, J., Douze, M., Jégou, H.: Billion-scale similarity search with GPUs. *IEEE Transactions on Big Data* **7**(3), 535–547 (2019)
19. Karpukhin, V., Oğuz, B., Min, S., Lewis, P., Wu, L.Y., Edunov, S., Chen, D., tau Yih, W.: Dense passage retrieval for open-domain question answering. EMNLP'2020 **ArXiv abs/2010.08191** (2020)
20. Kulkarni, H., MacAvaney, S., Goharian, N., Frieder, O.: Lexically-accelerated dense retrieval. In: Proc. of the 46th International ACM SIGIR Conference on Research and Development in Information Retrieval. p. 152–162. SIGIR '23, Association for Computing Machinery, New York, NY, USA (2023)
21. Kuzi, S., Zhang, M., Li, C., Bendersky, M., Najork, M.: Leveraging semantic and lexical matching to improve the recall of document retrieval systems: A hybrid approach. *arXiv preprint arXiv:2010.01195* (2020)
22. Lassance, C., Clinchant, S.: An efficiency study for splade models. SIGIR (2022)
23. Lewis, P., Oğuz, B., Xiong, W., Petroni, F., tau Yih, W., Riedel, S.: Boosted dense retriever. Proc. of NAACL pp. 3102–3117 (2022)
24. Li, H., Wang, S., Zhuang, S., Mourad, A., Ma, X., Lin, J., Zuccon, G.: To interpolate or not to interpolate: Prf, dense and sparse retrievers. SIGIR (2022)
25. Lin, J.J., Ma, X.: A few brief notes on deepimpact, coil, and a conceptual framework for information retrieval techniques. *ArXiv abs/2106.14807* (2021)
26. Liu, Z., Xiao, S., Shao, Y., Cao, Z.: RetroMAE-2: Duplex masked auto-encoder for pre-training retrieval-oriented language models. In: Rogers, A., Boyd-Graber, J., Okazaki, N. (eds.) *Proceedings of the 61st Annual Meeting of the Association for Computational Linguistics (Volume 1: Long Papers)*. pp. 2635–2648. Association for Computational Linguistics, Toronto, Canada (Jul 2023)
27. Ma, X., Wang, L., Yang, N., Wei, F., Lin, J.: Fine-tuning llama for multi-stage text retrieval (2023)
28. MacAvaney, S., Tonello, N., Macdonald, C.: Adaptive re-ranking with a corpus graph. In: Proc. of the 31st ACM International Conference on Information & Knowledge Management. p. 1491–1500. CIKM '22, Association for Computing Machinery, New York, NY, USA (2022)
29. Malkov, Y.A., Yashunin, D.A.: Efficient and robust approximate nearest neighbor search using hierarchical navigable small world graphs. *IEEE Trans. Pattern Anal. Mach. Intell.* **42**(4), 824–836 (apr 2020)
30. Mallia, A., Khattab, O., Tonello, N., Suel, T.: Learning passage impacts for inverted indexes. SIGIR (2021)
31. Mallia, A., Mackenzie, J., Suel, T., Tonello, N.: Faster learned sparse retrieval with guided traversal. In: Proceedings of the 45th International ACM SIGIR Conference on Research and Development in Information Retrieval. pp. 1901–1905 (2022)

32. Qiao, Y., Yang, Y., He, S., Yang, T.: Representation sparsification with hybrid thresholding for fast SPLADE-based document retrieval. *ACM SIGIR'23* (2023)
33. Qiao, Y., Yang, Y., Lin, H., Yang, T.: Optimizing guided traversal for fast learned sparse retrieval. In: *Proceedings of the ACM Web Conference 2023*. pp. 3375–3385 (2023)
34. Robertson, S.E., Zaragoza, H.: The probabilistic relevance framework: Bm25 and beyond. *Found. Trends Inf. Retr.* **3**, 333–389 (2009)
35. Shen, T., Geng, X., Tao, C., Xu, C., Huang, X., Jiao, B., Yang, L., Jiang, D.: LexMAE: Lexicon-bottlenecked pretraining for large-scale retrieval. In: *The Eleventh International Conference on Learning Representations (2023)*, <https://openreview.net/forum?id=PfpEtB3-csK>
36. Tan, S., Xu, Z., Zhao, W., Fei, H., Zhou, Z., Li, P.: Norm adjusted proximity graph for fast inner product retrieval. In: *Proceedings of the 27th ACM SIGKDD Conference on Knowledge Discovery & Data Mining*. p. 1552–1560. *KDD '21*, Association for Computing Machinery, New York, NY, USA (2021)
37. Thakur, N., Reimers, N., Rücklé, A., Srivastava, A., Gurevych, I.: BEIR: A heterogeneous benchmark for zero-shot evaluation of information retrieval models. In: *NeurIPS* (2021)
38. Touvron, H., Martin, L., Stone, K., Albert, P., Almahairi, A., Babaei, Y., Bashlykov, N., Batra, S., Bhargava, P., Bhosale, S., Bikel, D., Blecher, L., Ferrer, C.C., Chen, M., Cucurull, G., Esiobu, D., Fernandes, J., Fu, J., Fu, W., Fuller, B., Gao, C., Goswami, V., Goyal, N., Hartshorn, A., Hosseini, S., Hou, R., Inan, H., Kardas, M., Kerkez, V., Khabsa, M., Kloumann, I., Korenev, A., Koura, P.S., Lachaux, M.A., Lavril, T., Lee, J., Liskovich, D., Lu, Y., Mao, Y., Martinet, X., Mihaylov, T., Mishra, P., Molybog, I., Nie, Y., Poulton, A., Reizenstein, J., Rungta, R., Saladi, K., Schelten, A., Silva, R., Smith, E.M., Subramanian, R., Tan, X.E., Tang, B., Taylor, R., Williams, A., Kuan, J.X., Xu, P., Yan, Z., Zarov, I., Zhang, Y., Fan, A., Kambadur, M., Narang, S., Rodriguez, A., Stojnic, R., Edunov, S., Scialom, T.: *Llama 2: Open foundation and fine-tuned chat models* (2023)
39. Wang, L., Yang, N., Huang, X., Jiao, B., Yang, L., Jiang, D., Majumder, R., Wei, F.: SimLM: Pre-training with representation bottleneck for dense passage retrieval. *ACL* (2023)
40. Xiao, S., Liu, Z., Han, W., Zhang, J., Lian, D., Gong, Y., Chen, Q., Yang, F., Sun, H., Shao, Y., Deng, D., Zhang, Q., Xie, X.: Distill-VQ: learning retrieval oriented vector quantization by distilling knowledge from dense embeddings. *SIGIR* (2022)
41. Xiao, S., Liu, Z., Shao, Y., Cao, Z.: RetroMAE: pre-training retrieval-oriented transformers via masked auto-encoder. *EMNLP* (2022)
42. Yang, Y., Carlson, P., He, S., Qiao, Y., Yang, T.: Cluster-based partial dense retrieval fused with sparse text retrieval. In: *Proc. of the 47th International ACM SIGIR Conference on Research and Development in Information Retrieval*. p. 2327–2331. *SIGIR '24*, ACM, New York, NY, USA (2024)
43. Zhan, J., Mao, J., Liu, Y., Guo, J., Zhang, M., Ma, S.: Jointly optimizing query encoder and product quantization to improve retrieval performance. *CIKM* (2021)